Fabrication of metal-organic salts with heterogeneous conformations of ligand as dual-functional of urease and nitrification inhibitors

Wen-long Duan[a], Cong Ma[a], Jian Luan*[b], Fang Ding[d], Feng Yan[a], Lei Zhang*[c], Wen-Ze Li*[a]

[a] *College of Science, Shenyang University of Chemical Technology, Shenyang, 110142, P. R. China*

[b] *College of Sciences, Northeastern University, Shenyang, 110819, P. R. China*

[c] *Institute of Applied Ecology, Chinese Academy of Sciences. Shenyang, 110016, P. R. China*

[d] *College of Tourism and Resources Environment, Zaozhuang University, Zaozhuang, 277160, P. R. China*

Emails: wzli@syuct.edu.cn; 2010044@stu.neu.edu.cn; leizhang@iae.ac.cn

Table S1 Crystallographic data for MOSs **1**–**4**.

MOS	**1**	**2**	**3**	**4**
Empirical formula	$C_{30}H_{30}Cl_4CuF_4N_2$	$C_{30}H_{30}Cl_4F_4N_2Zn$	$C_{30}H_{30}CdCl_4F_4N_2$	$C_{30}H_{30}Cl_4CoF_4N_2$
Formula weight	699.90	701.73	748.76	695.29
Temperature (K)	298	298	298	298
Crystal size (mm)	0.14 × 0.13 × 0.10	0.14 × 0.12 × 0.10	0.14 × 0.12 × 0.09	0.14 × 0.12 × 0.10
Crystal system	Triclinic	Triclinic	Triclinic	Triclinic
Space group	*P*-1	*P*-1	*P*-1	*P*-1
Z	2	2	2	2
a (Å)	9.9316(5)	10.0080(5)	9.9952(6)	10.0083(5)
b (Å)	12.8000(6)	12.4928(6)	12.5695(8)	12.4895(6)
c (Å)	14.2699(7)	14.2889(7)	14.5331(9)	14.2962(7)
α (deg)	96.338(2)	93.920(2)	93.582(2)	93.778(2)
β (deg)	106.813(2)	107.938(2)	108.067(2)	108.137(2)
γ (deg)	112.103(2)	110.797(2)	111.162(2)	110.772(2)
V (Å^3)	1558.96(13)	1556.88(13)	1587.13(17)	1556.27(13)
D_x (mg cm^{-3})	1.491	1.497	1.567	1.484
μ (mm^{-1})	1.091	1.179	1.071	0.942
F(000)	714	716	752	710
R_{int}	0.0255	0.027	0.028	0.028
No. of collected data (unique)	28615	26072	18084	39078
No. of data with [I>=2σ (I)]	7744	7564	5360	12424
No.of parameters	370	358	358	370
S	1.022	1.107	1.052	1.055
R_f/wR_f	0.0408/0.1064	0.0521/0.1349	0.0534/0.1320	0.0582/0.1570
All data R_f/wR_f	0.0552/0.1173	0.0663/0.1470	0.0586/0.1367	0.0880/0.1807

[a] $R_1 = \Sigma||F_o|-|F_c||/\Sigma|F_o|$, [b] $wR_2 = \Sigma[w(F_o^2-F_c^2)^2]/\Sigma[w(F_o^2)^2]^{1/2}$.

Table S2 The hydrogen bonds (Å) and angles (°) for MOS **1**.

D–H···A	D–H (Å)	H···A (Å)	D···A (Å)	D–H···A (°)
N1–H1···Cl1(i)	0.980	2.154	3.079	156.61
N2–H2A···Cl3(ii)	0.980	2.232	3.165	158.62
C23–H23B···Cl4(iii)	0.987	2.652	3.563	156.51
C9–H9B···Cl2(iv)	0.971	2.719	3.676	169.00
C8–H8A···Cl2(v)	0.969	2.704	3.499	139.54
C16–H16···Cl4(vi)	0.930	2.924	3.598	130.44
C20–H20···Cl3(vii)	0.930	2.774	3.682	165.58
C13–H13···Cl3(viii)	0.931	2.708	3.571	154.54

Table S3 The hydrogen bonds (Å) and angles (°) for MOS **2**.

D–H···A	D–H (Å)	H···A (Å)	D···A (Å)	D–H···A (°)
N1–H1···Cl4(i)	0.980	2.118	3.076	165.28
N2–H2···Cl2(ii)	0.980	2.252	3.159	152.82
C15–H15A···Cl3(iii)	0.970	2.775	3.601	143.53
C16–H16B···Cl3(iv)	0.969	2.850	3.606	135.44
C30–H30B···Cl1(v)	0.968	2.823	3.725	155.28
C1–H1B···Cl3(vi)	0.970	2.925	3.800	150.61
C19–H19···Cl2(vii)	0.930	2.879	3.758	158.14
C8–H8B···Cl3(viii)	0.970	2.858	3.822	172.78

Table S4 The hydrogen bonds (Å) and angles (°) for MOS **3**.

D–H···A	D–H (Å)	H···A (Å)	D···A (Å)	D–H···A (°)
N1–H1···Cl3(i)	0.981	2.253	3.164	154.13
N2–H2···Cl1(ii)	0.980	2.114	3.077	167.18
C23–H23A···Cl2(iii)	0.970	2.898	3.726	143.93
C30–H30B···Cl2(iv)	0.970	2.784	3.648	148.80
C11–H11···Cl3(v)	0.930	2.833	3.733	163.75
C22–H22A···Cl2(vi)	0.970	2.884	3.851	175.30
C15–H15A···Cl2(vii)	0.970	2.905	3.787	151.72
C1–H1B···Cl4(viii)	0.969	2.841	3.750	156.68

Table S5 The hydrogen bonds (Å) and angles (°) for MOS **4**.

D–H···A	D–H (Å)	H···A (Å)	D···A (Å)	D–H···A (°)
N1–H1···Cl1(i)	0.980	2.251	3.157	153.25
N2–H2A···Cl4(ii)	0.980	2.115	3.072	165.14
C7–H7A···Cl2(iii)	0.970	2.932	3.803	149.91
C9–H9A···Cl2(iv)	0.970	2.848	3.607	135.72
C24–H24A···Cl2(v)	0.970	2.832	3.663	144.32
C23–H23B···Cl2(vi)	0.970	2.769	3.600	144.07
C8–H8A···Cl3(vii)	0.970	2.825	3.729	155.36
C12–H12···Cl1(viii)	0.930	2.871	3.749	158.05

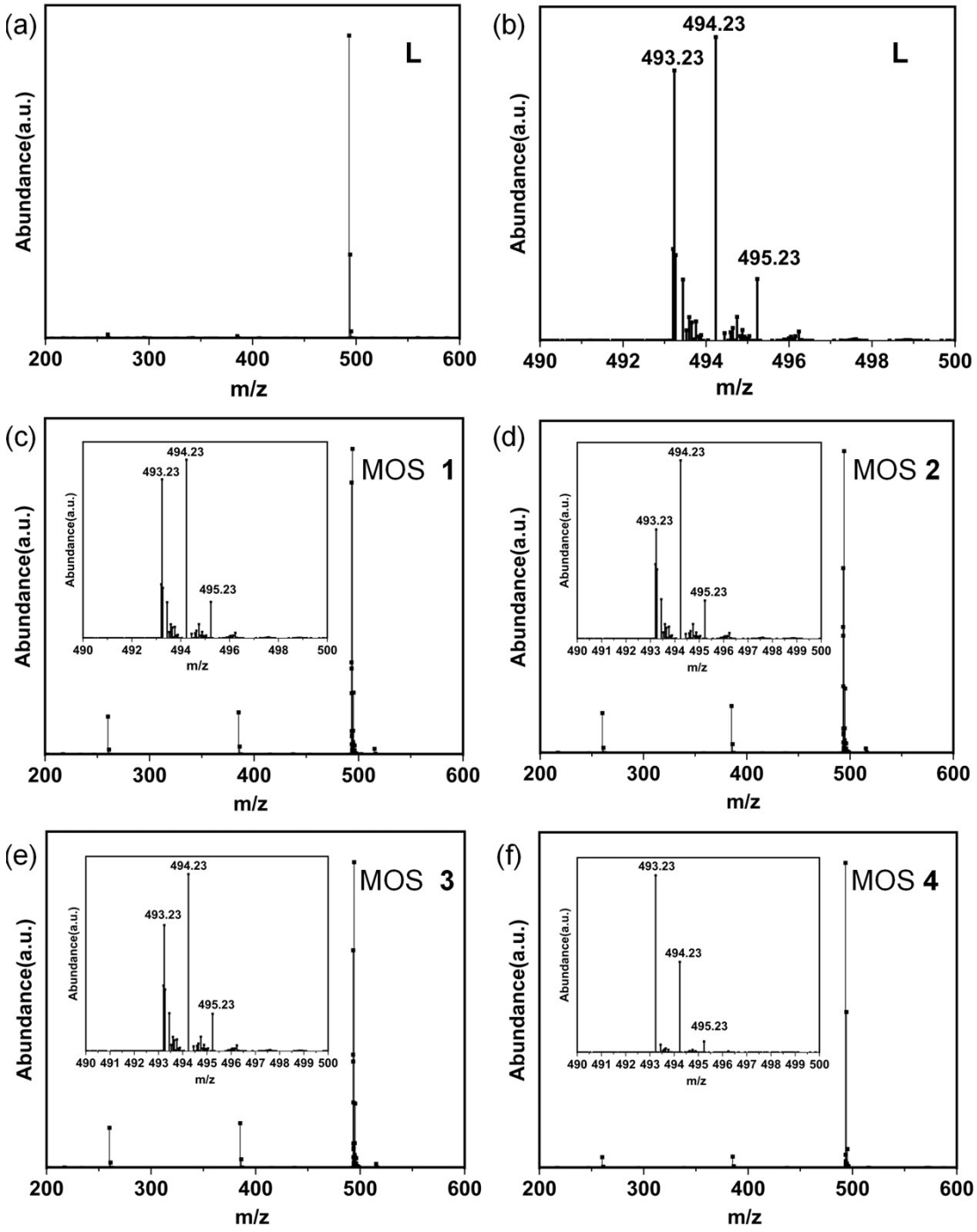

Fig. S1 The mass spectra of the **L** (a and b) and MOS **1** (c), **2** (d), **3** (e) and **4** (f).

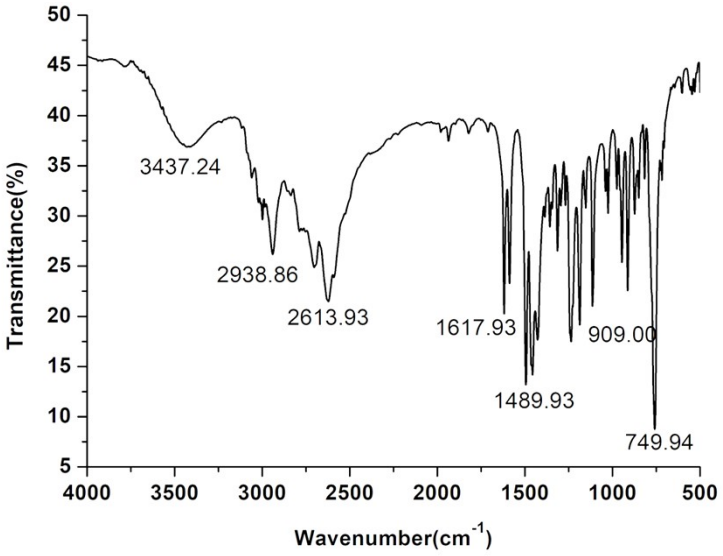

Fig. S2 IR spectrum of MOS **1**.

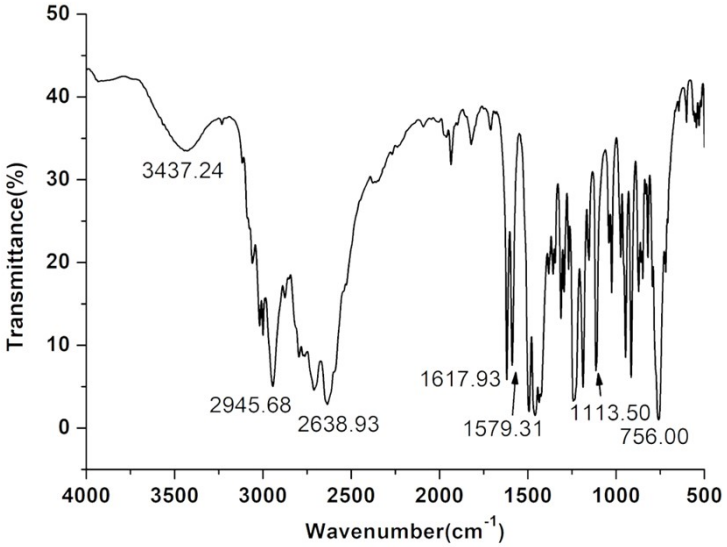

Fig. S3 IR spectrum of MOS **2**.

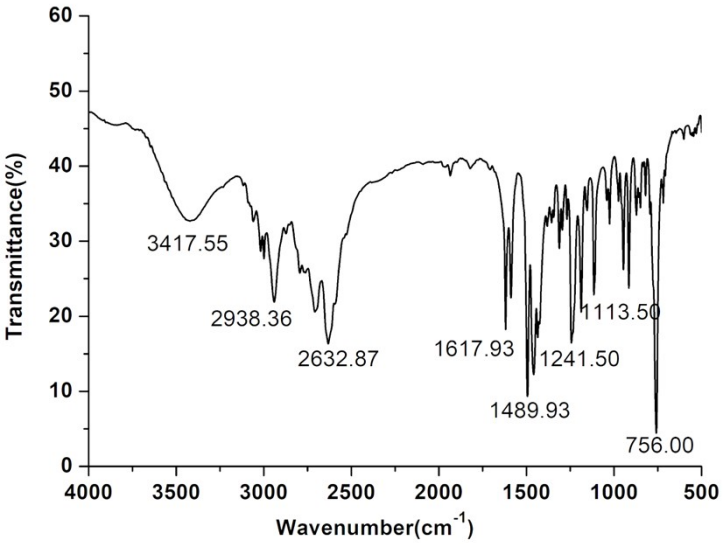

Fig. S4 IR spectrum of MOS **3**

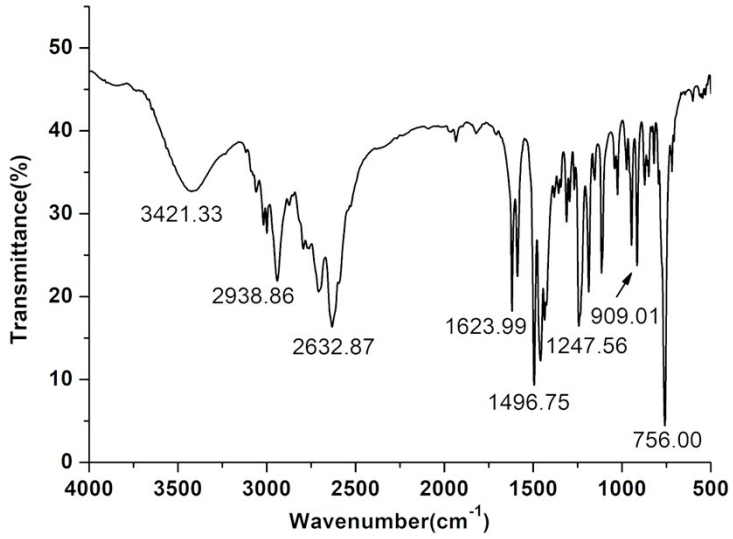

Fig. S5 IR spectrum of MOS **4**.

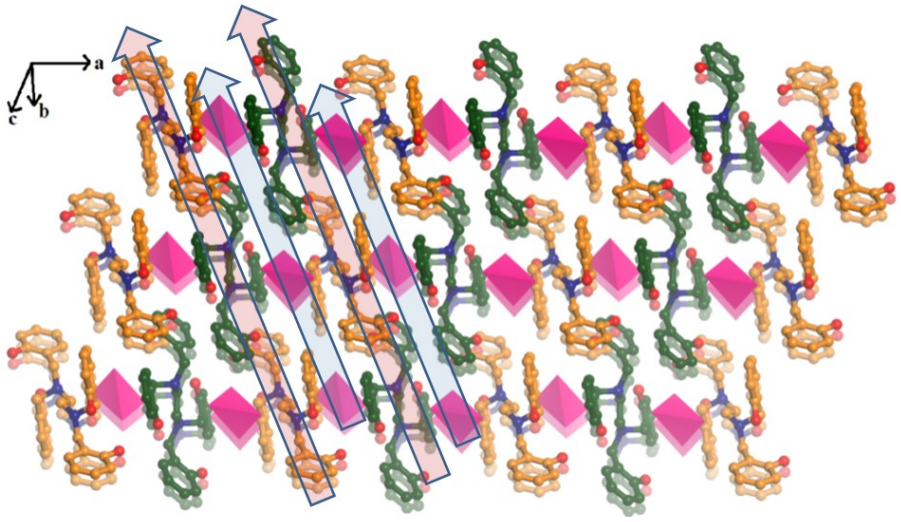

Fig. S6 3D packing of MOS **1**.

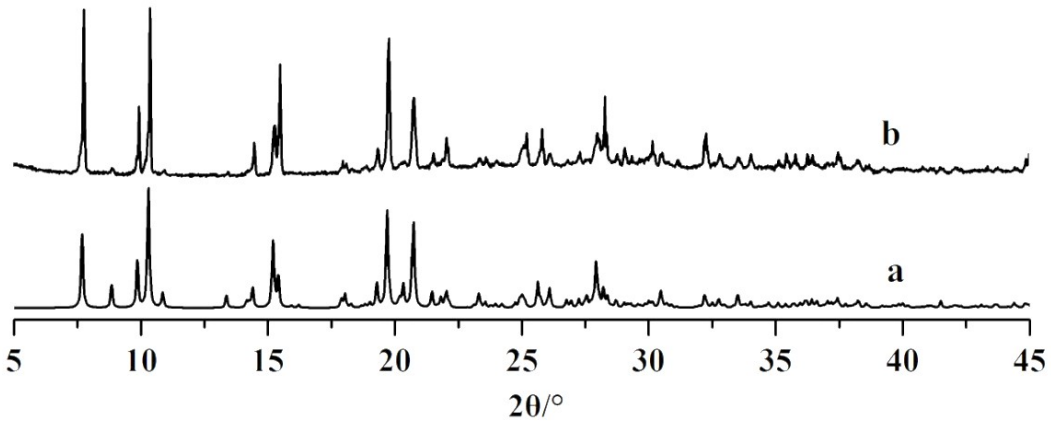

Fig. S7 Experimental (b) and simulated (a) PXRD patterns of MOS **1**.

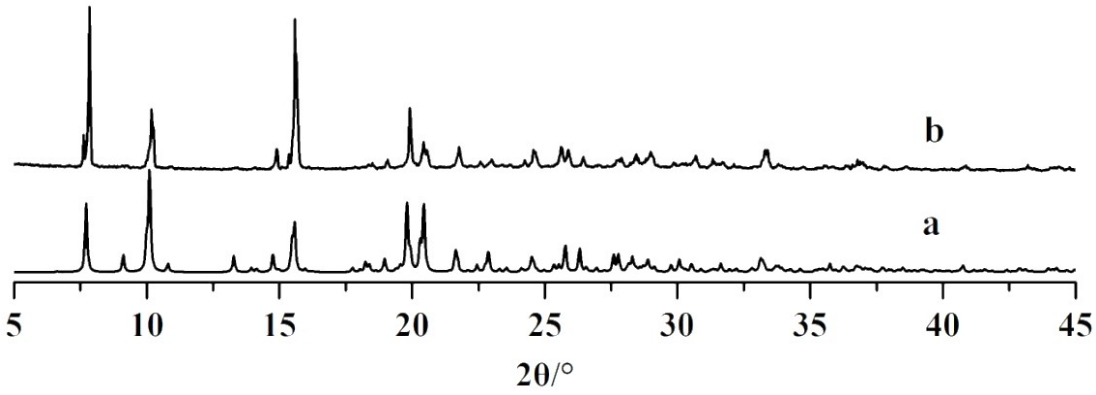

Fig. S8 Experimental (b) and simulated (a) PXRD patterns of MOS **2**.

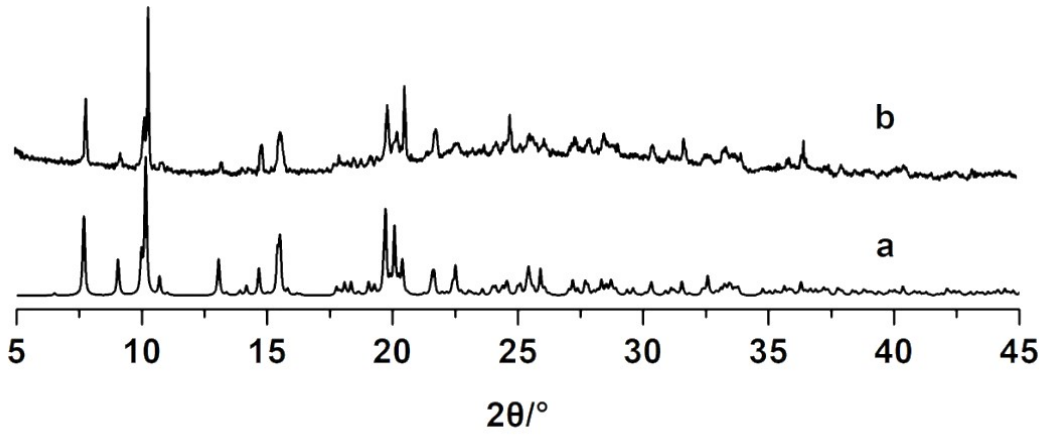

Fig. S9 Experimental (b) and simulated (a) PXRD patterns of MOS **3**.

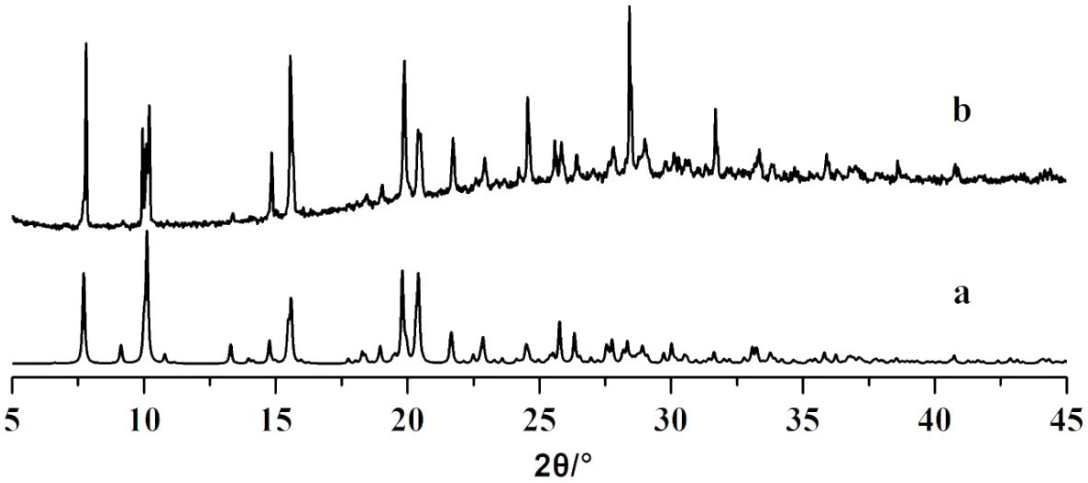

Fig. S10 Experimental (b) and simulated (a) PXRD patterns of MOS **4**.

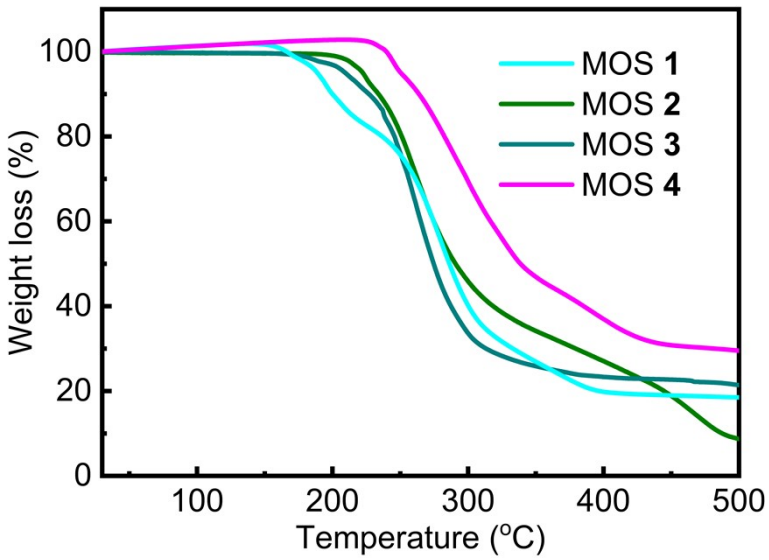

Fig. S11 TGA curves of MOSs **1**–**4**.

Table S6 Nitrification inhibitory of the tested materials.

Material	Day	Nitrification inhibition rate (%)
DCD	14	68.30%
L	14	8.12%
MOS **1**	14	65.29%
MOS **2**	14	48.68%
MOS **3**	14	26.12%
MOS **4**	14	20.76%
DCD	28	73.18%
L	28	34.03%
MOS **1**	28	70.75%
MOS **2**	28	13.29%
MOS **3**	28	—
MOS **4**	28	6.31%
DCD	37	74.80%
L	37	1.63%
MOS **1**	37	36.52%
MOS **2**	37	8.54%
MOS **3**	37	—
MOS **4**	37	4.91%
DCD	56	61.69%
L	56	—
MOS **1**	56	—
MOS **2**	56	11.01%
MOS **3**	56	—
MOS **4**	56	—
DCD	87	14.42%
L	87	—
MOS **1**	87	11.49%
MOS **2**	87	—
MOS **3**	87	8.89%
MOS **4**	87	—